Journal of King Saud University (Science) (2009) **21**, 109–117

King Saud University
Journal of King Saud University (Science)
www.ksu.edu.sa
www.sciencedirect.com

ORIGINAL ARTICLE

Application of single photon emission computed tomography (SPECT) parameters for bone scintigraphy

S.H.A. ALehyani

Physics Department, Faculty of Applied Science, Umm Al-Qura University, Makkah, Saudi Arabia

Received 15 February 2009; accepted 4 July 2009
Available online 5 August 2009

KEYWORDS

Radio-active wastes;
Arc plasma;
Vitrification;
Chemical analysis

Abstract The purpose of this study is to define an optimal strategy for tomographic acquisition procedure using single photon emission computed tomography (SPECT) phantom and apply it in routine bone scintigraphy studies. Acquisition parameters include the number of projections, matrix size; types of collimator used data and the multi-channel analyzer windows. This work demonstrates that, increasing number of views leads to better contrast and resolution of the reconstructed image due to increasing cancellation region of noise. The matrix size of 128×128 provides improvement in the resolution of the reconstructed image more than the 64×64 matrix although it takes more memory space in acquisition and takes longer time in processing the data. The ultra-high resolution collimator provides improvement in the resolution of the reconstructed image compared with the high resolution collimator. Energy window width 20% of the photo-peak energy gives the best contrast with adequate resolution in the reconstructed image than others energy window widths of 10% and 15% of the photo-peak energy. These could lead to an accurate investigation in the early detection of small metastatic lesions.

1. Introduction

Single photon emission computed tomography (SPECT) is a medical imaging modality that combines conventional nuclear medicine (NM) imaging technique and CT methods. Different from X-ray and CT, the SPECT uses radio-active labeled pharmaceuticals, i.e., radiopharmaceuticals, that distribute in different internal tissues or organs instead of an external X-ray source, the gamma photons emitted from the radio-active source are detected by radiation detectors similar to those used in conventional nuclear medicine. The SPECT method requires projection (or planar) image data to be acquired from different views around the patient. These projection data are subsequently reconstructed using image reconstruction methods that generate cross section images of the internally distributed radiopharmaceuticals. The SPECT images provide much improved contrast and detailed information about the radiopharmaceutical distribution as compared with the planar images obtained from conventional nuclear medicine methods (Craft and Tsui, 1995).

1018-3647 © 2009 King Saud University. All rights reserved. Peer-review under responsibility of King Saud University.
doi:10.1016/j.jksus.2009.07.004

Production and hosting by Elsevier

To produce quality emission tomographic images, the fundamental principles required to produce planar images must be employed along with those unique characteristics and principles of SPECT; these include instruments integrity, proper collimation, minimal source to detector distance and sufficient statistics (English and Brown, 1990). In a perfect imaging system, projections opposite each other are essentially mirror images of each other. Thus, the opposing views are mirror image and only one is needed. However, the nuclear medicine gamma camera is not a perfect imaging system, therefore, opposing views are not the same. First, the resolution of the gamma camera degrades as the distance between the camera and the object being imaged is increased. Second, a certain percentage of Compton scattered photons cannot be excluded owing to the finite energy resolution of the camera. Third, a certain fraction of gamma rays from an object is attenuated (absorbed) when they are emitted in an attenuating medium such as a patient. This phenomenon varies according to the depth of the attenuating medium between the object and gamma camera. In clinical SPECT, opposing projection views will never be the same. Therefore, the 360° arc is required for accurate reconstruction in most SPECT studies. One generally accepts exception to this rule in SPECT myocardial imaging, where the 180° acquisition is the standard practice. Although distortions due to variable and directionally resolution across the transverse slices in the 180° SPECT reconstruction will occur (Eisner et al., 1986), they are countered by the fact that the heart is generally positioned somewhat interiorly at the left in the thorax. Projection views opposite the heart see significantly less myocardial activity due to the attenuation through the patient's chest. Those views contribute mostly noise and scatter to the reconstruction, degrading overall resolution and contrast, while reconstruction from 180° acquisition will have improved resolution and contrast, at the expense of some distortion (Groch and Erwin, 2000).

1.1. Matrix size

The matrix size used to acquire the projection data plays a large part in the quality of the reconstructed image. The Nyquist theorem states that the highest spatial frequency in the image must be sampled at least twice to be accurately reproduced; i.e.:

$$\Delta X \leqslant \frac{1}{2} U_c$$

where U_c is the Nyquist frequency; ΔX is the spatial sampling interval or (pixel size).

Groch and Erwin show that the choice of matrix size depends on several factors. The size of a pixel should, ideally, be less than one third of the expected full-width at half maximum (FWHM) resolution of the SPECT system, measured at the center of rotation for the isotope where is being imaged, including the effects of the collimator and the radius of rotation (i.e., distance of camera from patient). In the SPECT system, where the camera's digital field of view (FOV with zoom = 1), the size of a pixel, D, in millimeters, may be calculated from (Groch and Erwin, 2000)

D = FOV/($Z \times N$)
FOV (mm) = the widest dimension of the computer image matrix
Z = zoom factor (e.g., 1.5, 2.0, etc.) during acquisition
N = number of pixels (e.g., 64 or 128) (Groch and Erwin, 2000).

When large matrices are used for smaller areas, higher resolution images can be obtained, but they have more statistical fluctuation (noise). Statistical fluctuation in large matrix size can be reduced by smoothing, but spatial resolution will decrease (Anthony et al., 2001).

1.2. Number of projections

Filtered back projection (FBP) is a technique used in nuclear medicine to reconstruct a slice from a set of its projection (Jain, 1989; Jalleau and Berche, 1983). The FBP technique uses a fast algorithm, but its streak artifact (or star artifact), which is present in the nuclear medicine modality, is a drawback. In nuclear medicine, this artifact is especially visible when a small region in the slice of interest contains high activity. The artifact is caused by the small number of acquired projections (in practice, usually equal to matrix size of the slice), whereas an infinite number of projections is theoretically required to perfectly reconstruct a slice. The mathematical formula of the FBP uses a Ramp filter, but usually, to reduce the streak artifact, this Ramp filter is replaced by a low-pass filter. This results in a loss of contrast and resolution in the reconstructed image. If the number of projections can be increased, the streak artifact is expected to be reduced without the drawbacks of a low-pass filter (Bruyant et al., 2000). Theoretically, for projection data acquired over a 180° arc, the number of projections required is dependent on the object diameter.

Where $D_{\max}$ is the number of linear samples (pixels) across the largest source diameter. The sampling distance is given by the linear dimension of one pixel. However, projection data in SPECT are acquired over a full 360° arc. the optimal number of projections in SPECT indicated by the above equation should therefore be doubled (Halama and Henkin, 1986).

1.3. Energy window

SPECT imaging is not ideal, however. Inherent in SPECT imaging is degradation which distorts the projection data. The essential source of degradation is the inclusion of scatter in the projections data. Compton scattering is the dominant mode of interaction. During Compton scattering the photons are reduced in energy and are deflected from their original path. Thus one can adjust the energy window to reduce the amount of scattered photons imaged, but not to eliminate scatter due to the presence of classically scattered photons and the finite energy resolution of current imaging system. The imaging of scattered photons degrades contrast and signal to noise ratio (SNR) and must be accounted for if attenuation compensation AC is to be accurate. The best way to reduce the effects of scatter would be to improve the energy resolution of the imaging systems by adjusting the NaI (TL) scintillator so that few scattered photons are acquired (Halama and Henkin, 1986).

1.4. Types of collimators

A collimator is a mechanical device used as a direction selector of photons incoming to the scintillation camera. The

collimator also defines the geometrical field of view of the camera as well as being the major contributor to the limited spatial resolution and to the low sensitivity of the system (Sorenson and Phelps, 1987). In the case of parallel hole collimators, only photons that are incident in a narrow solid angle, perpendicular to the collimator surface, will pass the collimator and interact in the scintillator. Consequently, it is possible to express the uniform spatial resolution and the uniform geometric efficiency of this collimator in terms of their physical dimensions. When conventional parallel hole collimators are used in SPECT, sources at a certain distance from the axis of rotation will contribute to the projection data with a collimator response that depends on the acquisition angle. As the projections are used in the reconstruction of the transverse images by means of, for example, filtered back projection, a variant non-isotropic blurring appears. The magnitude and characteristic of this non-isotropy are mainly a function of the distance from the center of rotation (COR), but other factors, such as the collimator hole length and the radius of rotation (ROR), also influence the non-isotropy.

2. Materials and methods

The gamma camera used in this study was the Sopha *DST-XLi*, which has dual detectors, and each detector head housed the NaI (TL) crystal and 94 photomultiplier tubes (*PMTs*) responsible for converting the incident gamma rays to electrical signals used to display patient images.

2.1. SPECT phantom

The SPECT phantom consists of a commercially supplied cylindrical Perspex container, internal diameter 180 mm and length 300 mm. The phantom has three distinct sections; the cold-rod section, a uniformity section and a hot rod section. Seven cold rods 80 mm long, have different diameters ranging from 35 mm to 9 mm. There are nine hot holes with diameters ranging from 30 mm to 3 mm. The long axis of all rods are aligned parallel to the long axis of the container. One end of the container is removable, as it is fixed with nylon screws and made water tight with a rubber o-ring. The top of the container has a screw filling plug. The total volume of the empty container is approximately 10.0 L and with the inserts in place the total fluid volume is about 6.0 L, with filled weight of approximately 13.0 kg. This phantom is designed to provide the periodic performance testing for the SPECT systems and is usually called Jaszczak phantom. It offers a single system for measuring resolution, slice thickness, linearity and uniformity. The phantom can be filled with a $^{99\,m}$Tc water solution having an activity of 15 mCi.

2.2. SPECT phantom imaging

For system performance, the SPECT phantom is filled with water containing approximately 555 MBq (15 mCi) of Tc-99 m. The radio-active material was mixed thoroughly by several shacking for about 15 min. It was turned up by inversion and then topped up to leave a small residual air bubble. The phantom was positioned on the gamma camera SPECT imaging table. The cylinder axis of the phantom was positioned parallel to the axis of rotation of the gamma camera detector, within the rotational field of view. SPECT acquisitions are then acquired to evaluate the different parameters. Acquisition parameters were established to represent the highest possible resolution as follows:

2.3. Acquisition parameters (acquisition protocol) used

[1] *Camera information*
Matrix size: 128×128; pixel size: 4.51 mm.
Magnification: 1.0; window width: 20%.
Collimator information: LEUHR.
[2] *Scan information*
Rotation type: step and shoot.
Orbit type: 25 cm.
No. of views: 128.
Time per acquisition (s): 20.

2.4. Acquisition parameters

2.4.1. Acquisition matrix size

The effect of matrix size type on SPECT images was studied. The SPECT phantom was used with fixed parameters for both acquisition and reconstruction. We recorded the data with a matrix size of 64×64 and a matrix size of 128×128.

The acquisition parameters were as in acquisition protocol [1], the only variable was in the matrix size

Matrix size: 64×64, 128×128.
Pixel size (mm): 9.02, 4.51.

2.5. Number of acquired views

In this study, the effect of the number of acquired views on SPECT images are evaluated. The SPECT phantom was imaged three times using fixed parameters in both acquisition and reconstruction. The only difference was the number of views per scan as we used 32, 64 and 128 views per each detector per study.

Acquisition parameters were as in acquisition protocol [1], but only variable was in the scan information. The number of views per each detector per scan was 32, 64 and 128 per study and angle step size (deg) changed, respectively.

2.6. Window width of multi-channel analyzer

In this study three acquisition of SPECT phantom images are acquired with three different window widths of the multi-channel analyzer: 10%, 15% and 20% for $^{99\,m}$Tc energy peak. We used fixed data in the three acquisition and reconstruction parameters. The only variable was the window of multi-channel analyzer (10%, 15% and 20%).

Acquisition parameters were as in the acquisition protocol [1], the variable was in the camera information window width: 10%, 15% and 20%.

2.7. Type of collimators

The effect of the collimator type on SPECT images was studied. The SPECT phantom was used with the fixed parameters for both acquisition and reconstruction. We recorded our data with low energy high resolution collimator (LEHR) and a low energy ultra-high resolution collimator (LEUHR).

Acquisition parameters were as in the acquisition protocol [1], the only variable was in the camera collimator: LEHR, LEUHR.

3. Results and discussion

3.1. Acquisition matrix size

Digital images are characterized by the matrix size and pixel depth. Matrix size determines the number and size of discrete picture elements and hence the degree of spatial details that can be presented. Higher SPECT resolution will be achieved with the smaller pixel size of 128×128 (pixel size = 4.51 mm) matrices than with a pixel size of 64×64 (pixel size = 9.02 mm) matrices. This can be achieved by using the SPECT phantom (Fig. 1). A line profile is taken through the cold holes of the SPECT phantom imaging with different matrix size (Fig. 2). However, the signal to noise ratio for the pixel may be much poorer as the image will have about 1/4 the counts per pixel of the 64×64 matrix. For the same acquisition, the image of the 128×128 matrix will have 1/5 the counts per pixel (Table 1). This means that for the same acquisition 128×128 matrix reconstructed percent noise more than 64×64 matrix. Also for the same number of projection views, 128×128 image acquisition will consume 4 times the disk space and computer memory, and the reconstructed volume will consume 8 times the disk space and memory, compared to the 64×64 image data. In addition, the 128×128 image data takes longer time in processing. Concerning the SPECT

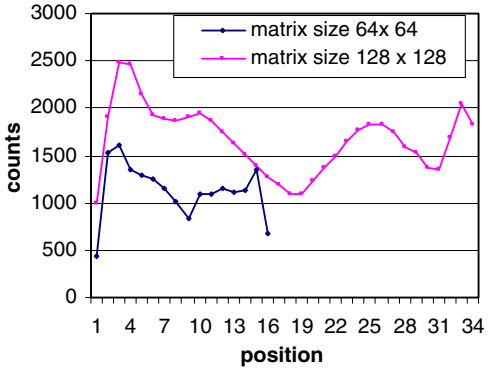

Figure 2 Shows the counts profile with respect to position for different matrix size.

resolution for perfect imaging gamma camera in the order 18–25 mm at the center of rotation, the matrix size 128×128 gives the best resolution, although matrix size 64×64 is perfectly adequate for most application.

3.2. Number of acquired views

Tomographic images reveal the internal distributions of radioactivity in three-dimensional objects, and thus allow anatomic localization and improve the contrast. Tomography requires a stable distribution of radionuclide, and a complete set of projections. In emission CT, a large number of measurements,

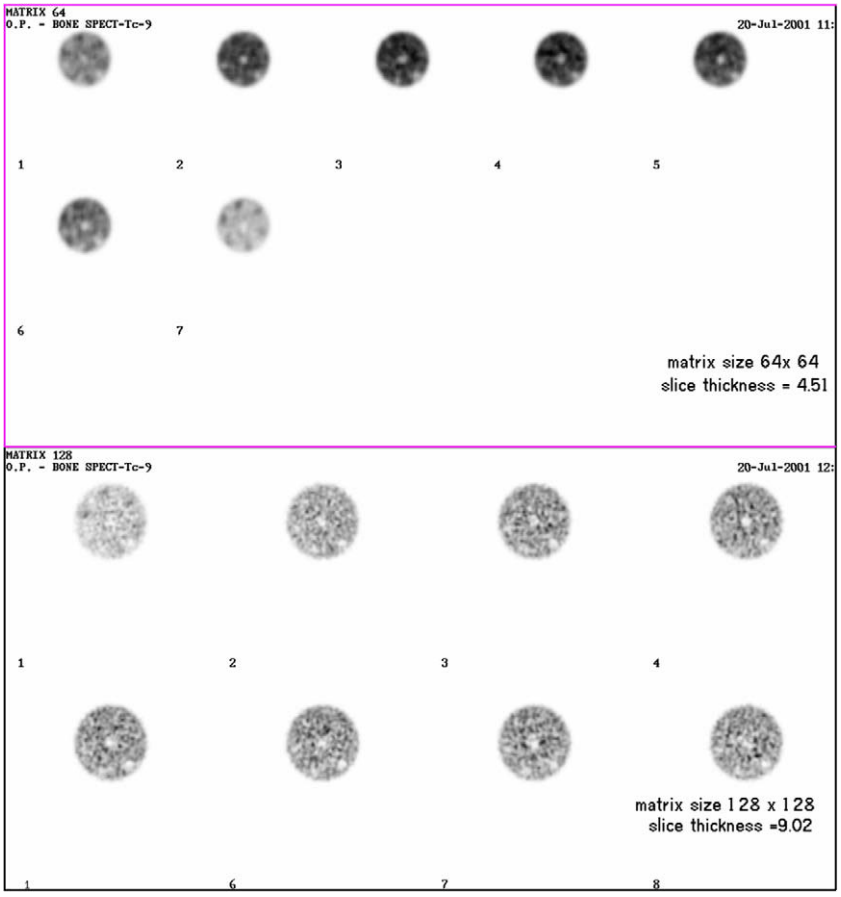

Figure 1 Transaxial image reconstruction of a cylindrical phantom filled with $^{99\,m}$Tc using different matrix sizes.

Table 1 The count variation of reconstructed slice with matrix size.

No. of slice	Matrix size 64 × 64			Matrix size 128 × 128		
	Counts	Max *x*, *y*	Max	Counts	Max *x*, *y*	Max
1	336,825	38, 16	1276	70,873	61, 30	118
2	350,139	30, 13	1265	66,121	77, 32	134
3	425,477	36, 19	1633	83,195	60, 40	136
4	435,509	36, 16	1470	96,695	66, 48	158
5	433,292	33, 18	1541	100,249	54, 41	143

called projections, are collected at various angles about patient during examination. This information is organized by the angles of acquisition into a stack, called a sinogram. Each projection is modified by applying a reconstruction filter (Ramp). These modified projections are back projected to form the transverse tomographic images. The quality of the tomographic image generated from filtered back projection depends on the number of acquired projections. For accurate reconstruction, the number of angular views over 360° should be at least equal to the projection image matrix size (e.g., 64 views for a 64 × 64 matrix and 128 views for the 128 × 128 matrix). When the number of views is less than the minimum, streak artifacts (image noise) may appear in the reconstructed slice. In SPECT phantom scan acquired with 32, 64 and 128, projections (Fig. 3), one can see that star artifacts (noise) are observed in the lower angular view and the image quality is decreased due to the limited collected counts and increasing noise. Taking a profile line through the *X*-axis of sphere holes

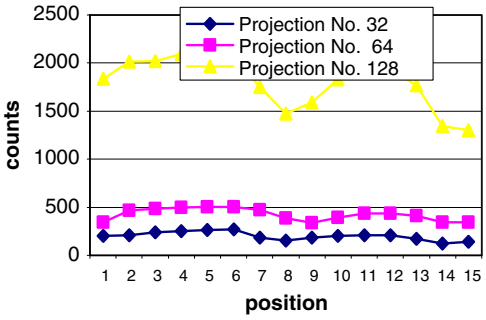

Figure 4 The counts profile with respect to position for different projection numbers.

of SPECT phantom including all projections views, we can see that the image resolution and contrast are improved with increasing the number of views (Fig. 4). This could be

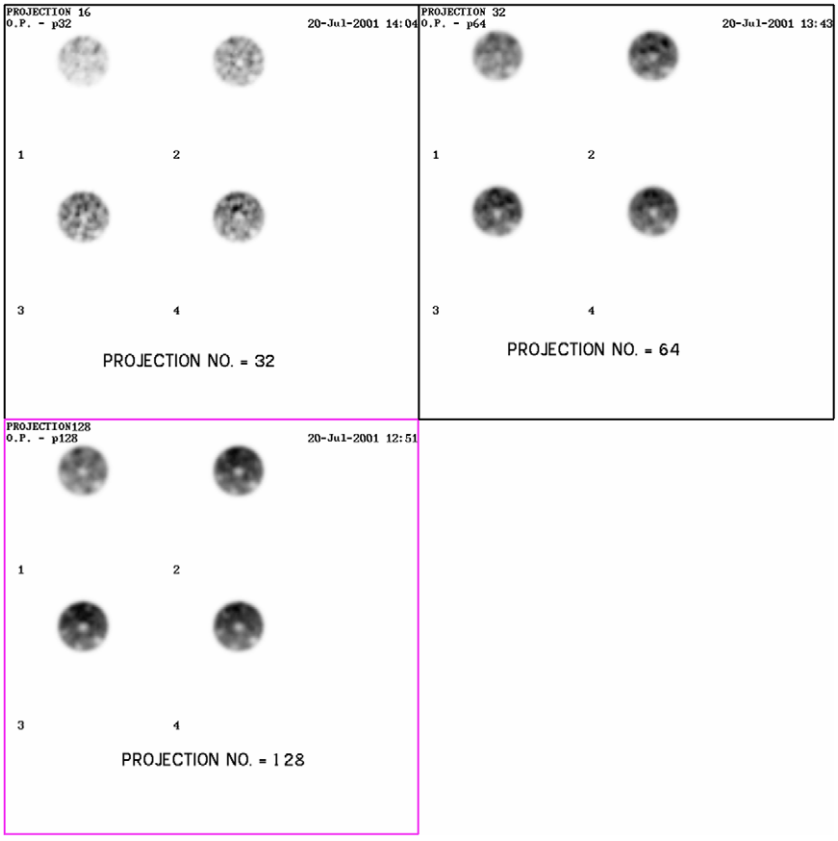

Figure 3 Transaxial image reconstruction of a cylindrical phantom filled with Tc-99 m with different projection numbers.

attributed to the region of cancellation of star artifacts being larger with a greater number of projection views used for back projection. The drawbacks of acquiring projections at an increasing number of angles are in the increasing data storage and computation requirements, of the computer, leading to an increasing study time since a significant amount of time is spent in moving the detector from one position to another.

3.3. Window width of multi-channel analyzer

The effect of energy window width on contrast and resolution of the image was measured using cold spheres of different sizes with different energy window widths of 10%, 15% and 20% of the photo-peak energy window for the 140 keV for $^{99\,m}$Tc (Fig. 5). With (10%) energy window there is reduction of counts (Table 2) due to the rejection of scattered photons giving an improve signal to noise ratio and resolution, while the contrast is degraded. For this reason we cannot visualize the cold spheres with low energy windows of 10% and 15% of the photo-peak energy. On the contrary, with an energy window of 20%, we notice an improvement in both resolution and contrast of the image due to more collected counts. By taking an activity profile through the cold spheres with different energy window widths (Fig. 6) we can demonstrate the cold

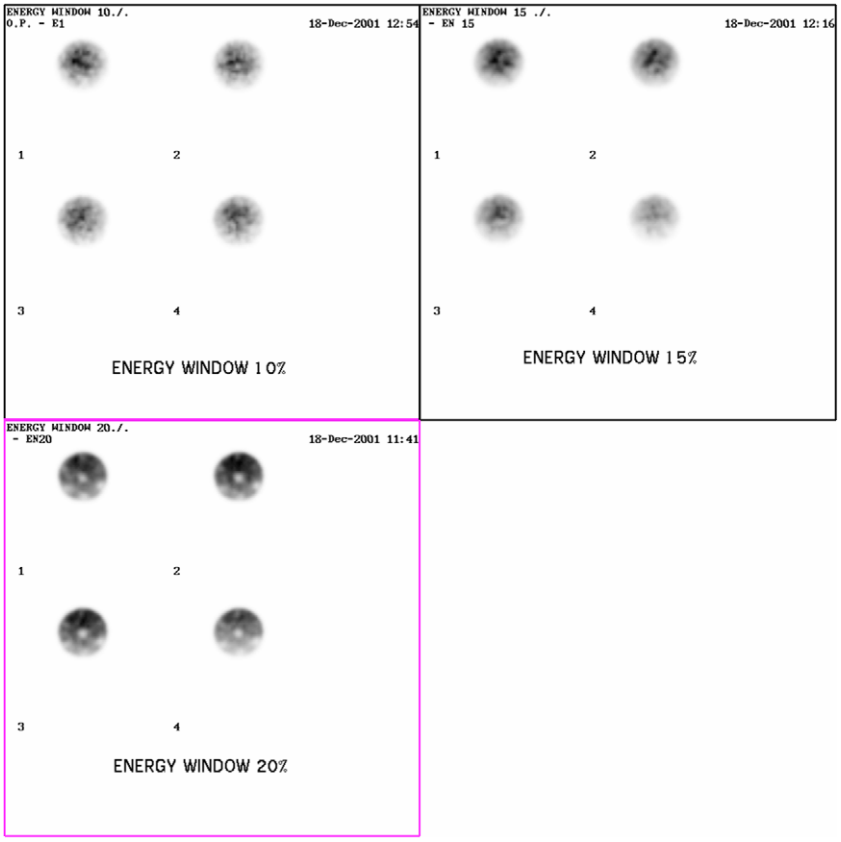

Figure 5 Transaxial image reconstruction of a cylindrical phantom filled with Tc-99 m with different energy window 10%, 15%, and 20% of the photo-peak energy.

Table 2 A comparison study for mean counts taken for different energy window.

Slice no.	Mean counts		
	Energy window 20%	Energy window 15%	Energy window 10%
1	100% (201.54)	81.785% (164.74)	46.2% (93.17)
2	100% (258.45)	81% (209.45)	45.56% (118.55)
3	100% (255.88)	79% (203.05)	44.12% (112.91)
4	100% (267.53)	77% (206.23)	42.1% (112.84)
5	100% (267.53)	77% (206.23)	42.1% (112.84)
6	100% (270.73)	77% (209.19)	42.1% (115.23)
7	100% (268.23)	77% (207.71)	43.16% (115.79)
8	100% (272.12)	78% (211.6)	43.3% (118.04)
9	100% (266.82)	78% (207.95)	43.3% (115.75)

() = pixel count per slice.

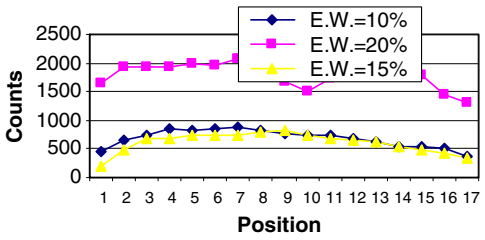

Figure 6 This figure shows the counts profile with respect to position for different energy window width.

spheres with the energy window of 20% than with the other windows of 15% or 10%. This means that with the energy window of 20% there is an improved contrast and adequate resolution than with the 15% and 10% windows.

3.4. Types of collimators

In SPECT studies, collimators of different spatial resolution and geometric efficiency are available for imaging. With selecting the appropriate collimator for SPECT use, there is a trade-off between spatial resolution, which can limit the contrast of the reconstructed image, and detection efficiency, which determines the noise in the image. In our study, we used two types of collimators to study their effect on the resolution of image using active rods of the SPECT phantom (Fig. 7). From this figure, the resolution between active rods decreases when the diameter of this rods is decreased for both types of collimators (LEUHRC and LEHRC) but the LEUHRC was able to separate small spheres (lesion) from each other better than LEHRC. The resolution is improved due to a reduction of scattered photons and statistical noise of the image taken by LEUHRC, where the diameter of the holes of this collimator

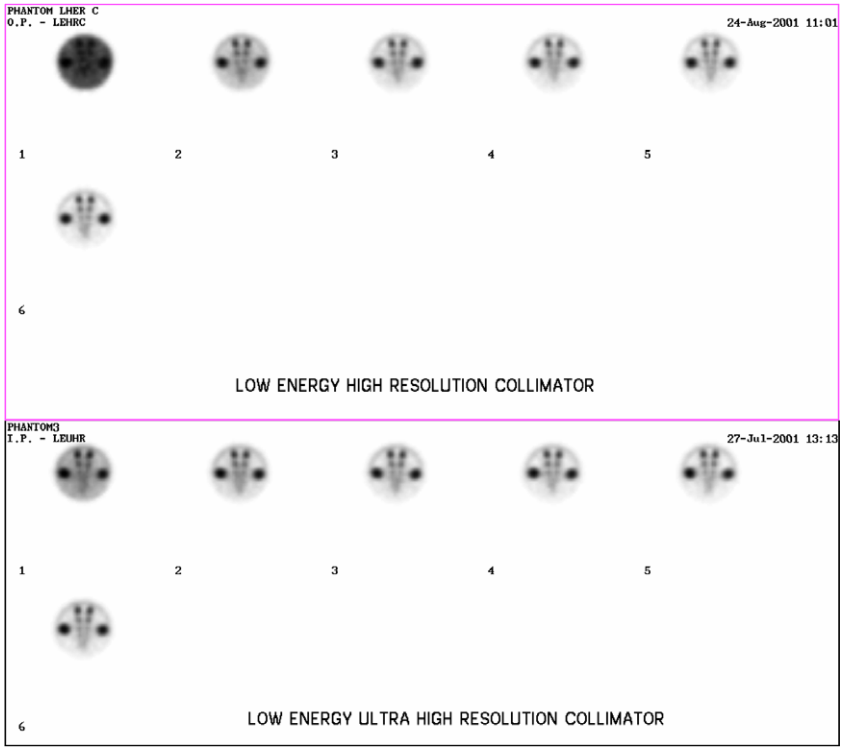

Figure 7 Transaxial image reconstruction of a cylindrical phantom filled with Tc-99 m using different types of collimators (LEUHRC and LEHRC).

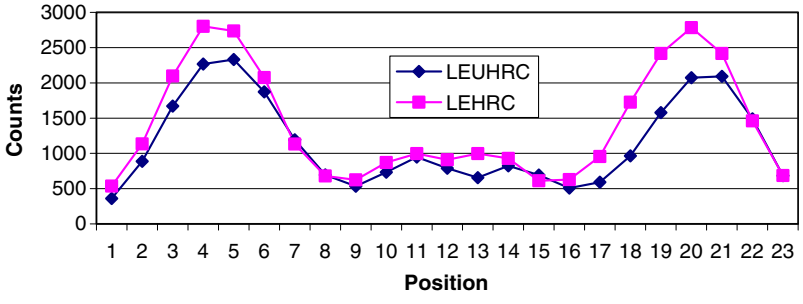

Figure 8 This figure shows the counts profile with respect to position for different type collimators.

is narrow and the septa thickness is large compared to LEHRC which affect the resolution parameter. Activity profiles drawn through the eight activity rods demonstrate the separation of the small sphere (lesion) in LEUHRC than in LEHRC (Fig. 8). The first three rods are well seen by both types of collimators. while the other rods are seen only by LEUHRC, Rods seven and eight are scarcely appreciable, because their diameters are too small for adequate separation. Also the edge artifacts on the phantom are greater in the image using the LEHRC. The LEUHRC is recommended in order to provide good spatial resolution. This could help when one is interested in imaging small lesion in bone scan imaging.

References

Anthony, P.J., Yester, M.V., Graham, S., Margaret, E., Andrew, E., Royal, H.D., 2001. Procedure Guideline for General Imaging. Society of Nuclear Medicine.

Bruyant, P.P., Jacques, S., Jeanjacques, M., 2000. Streak artifact reduction in filtered backprojection using a level line based interpolation method. J. Nucl. Med. 14, 1913–1919.

Craft, B.Y., Tsui, B.M.W., 1995. Nuclear medicine. In: Bronzino, J.D. (Ed.), Biomedical Engineering. New York, USA, pp. 1046–1037.

English, R.J., Brown, S.E., 1990. SPECT: Single Photon Emission Computed Tomography: A Primer. Society of Nuclear Medicine, New York, NY.

Eisner, R.L., Nowak, D.J., Pettigrew, R., 1986. Fundamentals of 180 degree acquisition and reconstruction in SPECT imaging. J. Nucl. Med. 27, 1717–1728.

Groch, M.W., Erwin, W.D., 2000. SPECT in the year 2000: basic principles. J. Nucl. Med. Technol. 28, 233–244.

Jain, A.K., 1989. Image reconstruction from projections. In: Kailath, T. (Ed.), Fundamentals of Digital Image Processing. Prentice-Hall, Englewood Cliffs, NJ, pp. 431–475.

Jalleau, M., Berche, C., 1983. Review of image reconstruction techniques in medical transaxial computed tomography. Ann. Radiol. 26, 13–22.

Halama, J.R., Henkin, R.E., 1986. Single photon emission computed tomography (SPECT). In: Freeman, L.M. (Ed.), Freeman and Johnson's Clinical Radionuclide Imaging. Grune Stratton, Inc., Orlando, USA, pp. 1530–1600.

Sorenson, J.A., Phelps, M.E., 1987. Physics in Nuclear Medicine, second ed. Grune & Stratton, Philadelphia, PA.

تطبيقات التصوير الطبقي باستخدام الفوتون أحادي الطاقة مخطط الوامضان العظمي

د/ سعود بن حميد بن أحمد اللحياني
كلية العلوم التطبيقية، قسم الفيزياء، جامعة أم القرى، مكة المكرمة
ص.ب 10130
(قدم للنشر في 1428/2/15هـ؛ وقبل للنشر في 1429/7/4هـ)

ملخص البحث. تهدف هذه الدراسة الي التعريف بأفضل إستراتيجية للحصول علي المعلومات الخاصة بالتصوير الطبقي، وذلك باستخدام الشبح المائي واستخدام الفوتون أحادي الانبعاث ومن ثم تطبيق هذه الإستراتيجية في القياسات اليومية الروتينية في تصوير العظام. وتتمثل الإستراتيجية في جمع المعلومات عن كلا من عدد الإسقاطات , حجم المصفوفة, أنواع المجمعات التي تستخدم في الحصول علي البيانات وقنوات التحليل الطيفي. ولقد تبين من خلال هذه الدراسة أنه عند زيادة عدد مقاطع التصويرية يؤدي ذلك إلي تباين أفضل ومن ثم تحليل أفضل للصورة المركبة وذلك بسبب الزيادة التي تطرأ علي حذف ضوضائية الصورة. وقد تبين أن المصفوفة 128×128 تعطي تحسنا ملحوظ في قوة التفريق مقارنة بالمصفوفة 64×64 بالرغم من أن المصفوفة 128×128 تشغل حيزا اكبر في الذاكرة وتستغرق وقت أطول في معالجة النتائج. كذلك تين ان المجمع ذى قوة التفريق العالية جدا يعطي تحسن ملحوظ في الصورة المركبة مقارنة بالمجمع ذي قوة التفريق العالية فقط.
أخير تبين أن نافذة الطاقة ذات عرض 20% من أقصي قيمة لطاقة الفوتون تعطي وضوح أفضل للصورة مع قوة تفريق مناسبة للصورة المركبة مقارنة بنوافذ الطاقة الأخرى ذات العرض 15% و10% من أقصي قيمة لطاقة الفوتون. كل ذلك يؤدي إلي فحص دقيق في الكشف الأولي للأورام السطحية الصغيرة غير الواضحة في العادة.